2-μm fluorescence and Raman spectra in high and low $Al(PO_3)_3$ content fluorophosphate glasses doped with Er-Tm-Ho

Meng Wang (王 孟)[1,2], Lixia Yi (衣丽霞)[1,2], Liyan Zhang (张丽艳)[1], Guonian Wang (汪国年)[1], Lili Hu (胡丽丽)[1], and Junjie Zhang (张军杰)[1*]

[1] *Key Laboratory of Material Science and Technology for High Power Lasers, Shanghai Institute of Optics and Fine Mechanics, Chinese Academy of Sciences, Shanghai 201800, China*

[2] *Graduate School of Chinese Academy of Sciences, Beijing 100039, China*

[*] *E-mail: jjzhang@mail.siom.ac.cn*

Received February 20, 2009

Thermal stability and 2-μm fluorescence of high and low $Al(PO_3)_3$ content of fluorophosphate glasses are investigated. Thermal stability of high $Al(PO_3)_3$ content of fluorophosphate glass is better than low $Al(PO_3)_3$ content of fluorophosphate glass. However, 2.04-μm fluorescence intensity of high $Al(PO_3)_3$ content of fluorophosphate glass is only 48.2, lower than low $Al(PO_3)_3$ content of fluorophosphate glass. Raman spectroscopy is employed to investigate the difference in thermal stability and 2-μm fluorescence. Moreover, fluorescence peak intensity ratios of 2.04 to 1.81 μm and 2.04 to 1.57 μm are calculated, which indicate that Er-Tm-Ho doped fluorophosphate glasses are suitable materials in 2-μm applications.

OCIS codes: 160.5690, 160.4670, 300.6280, 160.2750.

doi: 10.3788/COL20090711.1035.

2-μm region laser emission has drawn considerable attention because of its numerous potential applications including remote sensing, eye-safe laser lidar, and biomedical applications[1−4]. In recent years, there are many reports of fluoride glasses operating in 2-μm region[5,6], but the unsatisfactory chemical and environmental stability limits their application. Fluorophosphate glasses, which possesses the merits of both fluoride and phosphate glasses, is an interesting candidate for 2-μm region fiber and other optical material applications. According to the recent research[7], the physical and chemical properties of fluorophosphate glasses compare well against fluoride glasses, and its maximum phonon energy which is smaller than phosphate glasses, can lead to low nonradiative relaxation in fluorophosphate glasses benefitting to 2-μm region. Meanwhile, they are characterized with extensive compositions, complicated network constructions, and high content of doped rare earth ions[8,9]. All the favorable properties make them suitable to develop rare earth doped optical materials.

However, the different phosphate content in fluorophosphate glasses engenders distinct effect on physical, chemical, and optical properties. This letter aims to investigate the effect of high phosphate content (20-mol% $Al(PO_3)_3$) and low phosphate content (5-mol% $Al(PO_3)_3$) on thermal stability, 2-μm fluorescence, and structure in Er-Tm-Ho doped fluorophosphate glasses.

The studied fluorophosphate glasses were prepared in compositions: $20Al(PO_3)_3$-$13MgF_2$-$47BaF_2$-$13LiF$-$4ErF_3$-$2TmF_3$-$1HoF_3$(mol%) named FHP where the F/P ratio is 2.6 and $5Al(PO_3)_3$-$32AlF_3$-$10MgF_2$-$15CaF_2$-$7SrF_2$-$14BaF_2$-$10NaF$-$4ErF_3$-$2TmF_3$-$1HoF_3$ (mol%) named FLP where the F/P ratio is 14.8. All started materials were of analytical grade. About thirty-gram batches of powders were weighed and mixed thoroughly, and then placed into a platinum crucible and melt at 1000–1080 °C for 30 min. After completely melting and fining, the glass liquid was cast into graphite moulds, and then annealed for several hours at the glass transition temperature before they were cooled to room temperature at a rate of 20 °C/h. Finally, the annealed samples were cut and polished with the size of 15×10×1.5 (mm) for optical measurements.

The characteristic temperatures (temperature of glass transition T_g, temperature of onset crystallization peak T_x, and temperature of top crystallization peak T_p) were determined by differential scanning calorimetry (DSC) using NETZSCH STA 409PC. The fluorescence spectra were measured with a Triax 550 type spectrometer (Jobin-Yvon Co., France) upon excitation of 808-nm laser diode (LD) in the range of 1.4 – 2.2 μm. The Raman spectra were measured using Micro Raman Spectra Lab Ram-1B. All the measurements were performed at room temperature.

The typical DSC graphs of FHP and FLP samples are represented in Fig. 1. The characteristic temperatures are listed in Table 1. ΔT, defined as the temperature gap between T_x and T_g, is often used as a measure of thermal stability of glass. With the increase of ΔT, the thermal stability of glass changes to be better. Table 1 shows that ΔT of FHP glass sample is 129 °C, and it is a little larger than that of FLP sample. According to the research of Lebullenger[10], characteristic temperature of glass was correlated with breaking of the chemical bonds by thermal motion. Comparing with FLP sample, high phosphate content in FHP sample increases the strength of the average chemical bond or produces a more linked or interconnected glass network, and enhances the thermal stability of fluorophosphate glass. Therefore, FHP sample possesses a little better thermal stability than

FLP glass sample. However, no matter high or low the phosphate content of fluorophosphate glasses is, the thermal stability is more desirable than fluoride glasses whose ΔT is 89 °C[11], and it is obviously important in glass bulk or fiber fabrication.

Figure 2 presents the fluorescence spectra of an Er-Tm-Ho doped FHP and FLP samples pumped by an 808-nm laser. In the spectra, it can be found that three fluorescence bands center at near 2.04, 1.81 and 1.57 μm, corresponding to the emission from the excited states Ho^{3+}: $^5I_7$, Tm^{3+}: $^3F_4$, and Er^{3+}: $^4I_{13/2}$ to the ground states. FLP sample shows stronger 2.04-μm fluorescence than FHP sample, whereas the 1.81- and 1.57-μm fluorescence intensities are a little lower, and the intensity values are listed in Table 2. In addition, Table 2 also shows the peak intensity ratios of 2.04 to 1.81 μm and 2.04 to 1.57 μm. The ratios $I_{2.04}/I_{1.81}$ and $I_{2.04}/I_{1.57}$ of FLP sample can reach to 7.2 and 19.8 respectively, and are much higher than those of FHP sample. The results indicate that the energy of Tm^{3+} and Er^{3+} ions in Er-Tm-Ho doped FLP sample can transfer more sufficiently to Ho^{3+} ions than FHP sample, leading to stronger 2-μm fluorescence. From the ratios, it is also worthwhile to mention that in Er-Tm-Ho doped fluorophosphate glasses, the 2.04-μm fluorescence is so intense that the 1.81-and 1.57-μm fluorescence can be ignored, and this

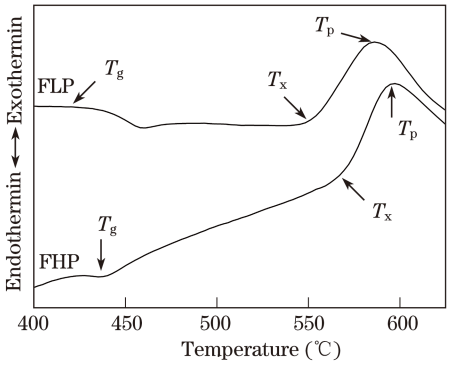

Fig. 1. DSC graphs of FHP and FLP samples.

Table 1. Characteristic Temperatures of FHP and FLP Samples

Glass Samples	T_g (°C)	T_x (°C)	T_p (°C)	ΔT (°C)
FHP	435	564	597	129
FLP	429	555	586	126

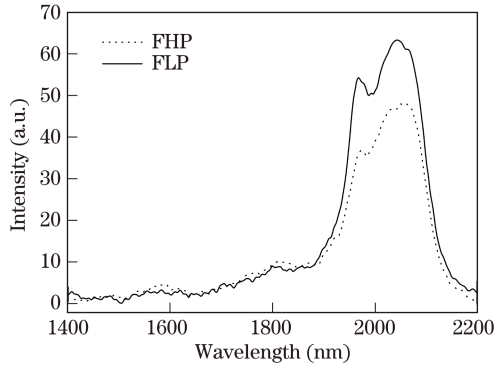

Fig. 2. Fluorescence spectra of Er-Tm-Ho doped FHP and FLP samples pumped by an 808-nm laser.

Table 2. Fluorescence Intensities and Intensity ratios of FHP and FLP Samples pumped by an 808-nm Laser

Glass Samples	$I_{2.04}$	$I_{1.81}$	$I_{1.57}$	$I_{2.04}/I_{1.81}$	$I_{2.04}/I_{1.57}$
FHP	48.2	10.2	4.7	4.7	10.3
FLP	63.2	8.8	3.2	7.2	19.8

phenomenon is significant in the 2-μm region fluorescence research. Consequently, Er-Tm-Ho doped FLP sample is a more suitable material than FHP sample in 2-μm region application.

The pumping scheme and energy transfer process of Er-Tm-Ho doped fluorophoshpate glasses are illustrated in the energy level diagram of Fig. 3. Comparing with Tm-Ho doped glasses, Er-Tm-Ho doped glasses also have effective sensitization effect while there are a few reports about that. From Fig. 3, Er^{3+} and Tm^{3+} ions both can absorb the 808-nm pumping beam, and the energy sufficiently transfers form Er^{3+}: $^4I_{13/2}$ and Tm^{3+}: $^3F_4$ levels to Ho^{3+}: $^5I_7$ level, finally the strong 2.0-μm fluorescence can be obtained.

The Raman spectra of FHP and FLP glass samples are shown in Fig. 4. Nine bands labeled a – i are defined. Band a is observed clearly in the spectra of FHP and FLP samples, and it is related to M – F (M = Mg^{2+}, Ba^{2+} in FHP sample and M = Mg^{2+}, Ca^{2+}, Sr^{2+}, and Ba^{2+} in FLP sample) bond vibration[10]. Band b is only observed in the spectrum of FLP sample and ascribed to $[AlF_4]$ vibration[12]. Band c is observed in the spectrum of FHP sample and can be related to the symmetric stretching of P–O–P in metaphosphate tetrahedron[13]. Band d in the spectrum of FLP sample is due to the symmetric vibration of terminal groups of $(-OPO_2F)^{2-}$[14]. Band e can be observed clearly in the spectrum of FHP sample, while there is a little shoulder in the spectrum of FLP sample which is also assumed to be band e. It is attributed to the symmetric stretching of F–P–F in $(PO_2F_2)^-$ group[15]. In the spectrum of FLP sample, the strongest peak appears at 1012 cm^{-1} defined as band f, which presents as a shoulder in the spectrum of FHP sample. It is ascribed to O–P–F stretching vibration in the $(PO_3F)^{2-}$ group[16]. However, the strongest peak in the spectrum of FHP sample is observed at 1049 cm^{-1} defined as band g and related to the symmetric stretching of O–P–O in $P_2(O, F)_7$ group[15]. Band h can be both observed in the spectra of FHP and FLP samples and is attributed to the

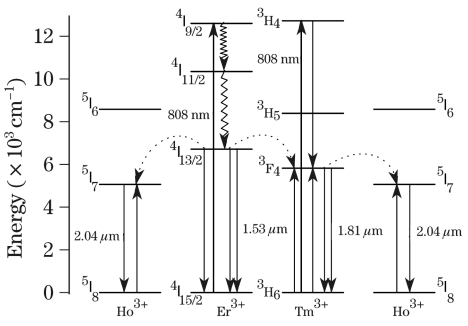

Fig. 3. Energy level diagram and energy transfer sketch map of Er-Tm-Ho doped fluorophosphate glasses pumped by an 808-nm laser.

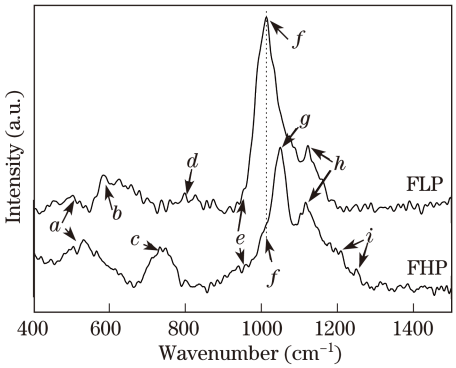

Fig. 4. Raman spectra of FHP and FLP samples.

symmetric stretching vibration of O–P–O in metaphosphate tetrahedron[13]. Band i only presents in the spectrum of FHP sample and is due to the asymmetric stretching of non-bridging oxygen in O–P–O[13]. Based on the results of the Raman spectra, the maximum phonon energy of FLP sample is smaller than FHP sample. According to the report of Peng[17], the fluorescence intensity of Ho^{3+}:$^5I_7 \rightarrow {}^5I_8$ transition is mainly controlled by the quantum efficiency driven primarily by the phonon energy. The higher maximum phonon energy leads to the larger nonradiative relaxation, and depresses the fluorescence intensity. Consequently, the 2.04-μm fluorescence intensity of FLP sample is stronger than FHP sample. In addition, the structure of FHP sample is mainly affected by the symmetric stretching of O–P–O in $P_2(O, F)_7$ group, and the larger number of O–P–O in FHP sample maybe results in that the thermal stability of FHP glass sample is better than that of FLP sample.

Therefore, from the comparative 2-μm fluorescence of FHP and FLP samples, the low phosphate content of fluorophosphate glasses should be chosen, although the thermal stability is a little worse than the high phosphate content of fluorophosphate glasses. Moreover, in order to achieve the most sufficient and intense 2-μm fluorescence, the optimization of rare earth ions doped concentration should be investigated in further study.

In this letter, the thermal stability 2-μm fluorescence and Raman spectra of high and low phosphate content of Er-Tm-Ho doped fluorophosphate glasses are investigated and compared. Low phosphate content of fluorophosphate glass possesses much stronger 2-μm fluorescence and a little worse thermal stability than high phosphate content of fluorophosphate glass. From the Raman analysis, the comparative results of thermal stability and 2-μm fluorescence are correlated to the difference of the maximum phonon energy. From the study, low phosphate content of fluorophosphate glasses should be chosen for 2-μm region applications.

This work was supported by the National "863" Project of China (No. 2007AA03Z441) and the National Natural Science Foundation of China (Nos. 50572110 and 60607014).

References

1. K. Scholle, E. Heumann, and G. Huber, Laser Phys. Lett. **1,** 285 (2004).
2. Y. Li, Y. Ju, Y. Urata, and Y. Wang, Chin. Opt. Lett. **5,** 351 (2007).
3. Y. Tsang, B. Richards, D. Binks, J. Lousteau, and A. Jha, Opt. Express **16,** 10690 (2008).
4. Y. Tang, Y. Yang, X. Cheng, and J. Xu, Chin. Opt. Lett. **6,** 44 (2008).
5. J. L. Doualan, S. Girard, H. Haquin, J. L. Adam, and J. Montagne, Opt. Mater. **24,** 563 (2003).
6. S. D. Jackson, Electron. Lett. **37,** 821 (2001).
7. M. Wang, L. Yi, Y. Chen, C. Yu, G. Wang, L. Hu, and J. Zhang, Mater. Chem. Phys. **114,** 295 (2009).
8. J. F. Philipps, T. Töpfer, H. Ebendorff-Heidepriem, D. Ehrt, and R. Sauerbrey, Appl. Phys. B **72,** 399 (2001).
9. M. Liao, L. Hu, Y. Fang, J. Zhang, H. Sun, S. Xu, and L. Zhang, Spectrochim. Acta Part A **68,** 531 (2007).
10. R. Lebullenger, L. A. O. Nunes, and A. C. Hernandes, J. Non-Cryst. Solids **284,** 55 (2001).
11. C. Yu, J. Zhang, and Z. Jiang, J. Non-Cryst. Solids **353,** 2654 (2007).
12. L. Koudelka, J. Klikorka, M. Frumar, M. Pisářeik, V. Kellö, V. D. Khalilev, V. I. Vakhrameev, and G. D. Chkhenkeli, J. Non-Cryst. Solids **85,** 204 (1986).
13. R. K. Brow and D. R. Tallant, J. Non-Cryst. Solids **222,** 396 (1997).
14. V. Sudarsan and S. K. Kulshreshtha, J. Non-Cryst. Solids **258,** 20 (1999).
15. J.-J. Videau, J. Portier, and B. Piriou, J. Non-Cryst. Solids **48,** 385 (1982).
16. J. Y. Ding, P. Y. Shih, S. W. Yung, K. L. Hsu, and T. S. Chin, Mater. Chem. Phys. **82,** 61 (2003).
17. B. Peng and T. Izumitani, Opt. Mater. **4,** 797 (1995).